

**Development of Endothelium-Denuded Human Umbilical Veins as Living Scaffolds for Tissue-Engineered Small Caliber Vascular Grafts**

Journal:	<i>Journal of Tissue Engineering and Regenerative Medicine</i>
Manuscript ID:	TERM-11-0069.R1
Wiley - Manuscript type:	Research Article
Date Submitted by the Author:	n/a
Complete List of Authors:	<p>Hoernicka, Markus; University of Regensburg Medical Center, Department of Cardiothoracic Surgery                      Schrammel, Siegfried; University of Applied Sciences Regensburg, FB Maschinenbau                      Bursa, Jiri; Brno University of Technology, Institute of Solid Mechanics, Mechatronics and Biomechanics                      Huber, Georgine; University of Regensburg, Krankenhaus Barmherzige Brüder, Klinik St. Hedwig, Department of Obstetrics and Gynecology                      Bronger, Holger; Technical University Munich, Frauenklinik (OB/GYN)                      Schmid, Christof; University of Regensburg Medical Center, Department of Cardiothoracic Surgery                      Birnbaum, Dietrich; University of Regensburg Medical Center, Department of Cardiothoracic Surgery</p>
Keywords:	vascular tissue engineering, small caliber vessel graft, endothelium, biomechanics, human umbilical vein, bioreactor

SCHOLARONE™  
Manuscripts

1  
2  
3  
4  
5  
6  
7  
8  
9  
10  
11  
12  
13  
14  
15  
16  
17  
18  
19  
20  
21  
22  
23  
24  
25  
26  
27  
28  
29  
30  
31  
32  
33  
34  
35  
36  
37  
38  
39  
40  
41  
42  
43  
44  
45  
46  
47  
48  
49  
50  
51  
52  
53  
54  
55  
56  
57  
58  
59  
60

# Development of Endothelium-Denuded Human Umbilical Veins as Living Scaffolds for Tissue-Engineered Small Caliber Vascular Grafts

Markus Hoenicka\*<sup>1</sup>, Siegfried Schrammel<sup>2</sup>, Jiri Bursa<sup>3</sup>, Georgine Huber<sup>4</sup>, Holger Bronger<sup>5</sup>, Christof Schmid<sup>1</sup>, Dietrich E Birnbaum<sup>1</sup>

<sup>1</sup>University of Regensburg Medical Center, Department of Cardiothoracic Surgery, Regensburg, Germany <sup>2</sup>University of Applied Sciences Regensburg, FB Maschinenbau, Regensburg, Germany

<sup>3</sup>Brno University of Technology, Institute of Solid Mechanics, Mechatronics and Biomechanics, Brno, Czech Republic <sup>4</sup>University of Regensburg, Krankenhaus Barmherzige Brüder, Klinik St. Hedwig, Department of Obstetrics and Gynecology, Regensburg, Germany

<sup>5</sup>Technical University Munich, Frauenklinik (OB/GYN), Munich, Germany

\* corresponding author: Markus Hoenicka, PhD, University of Regensburg Medical Center, Department of Cardiothoracic Surgery, Franz-Josef-Strauss-Allee 11, 93053 Regensburg, Germany. Phone ++49-941-944-9901 Fax ++49-941-944-9902 email

markus.hoenicka@klinik.uni-regensburg.de

**Abstract**

Tissue engineered small caliber vessel grafts may help to alleviate the lack of graft material for coronary and peripheral bypass grafting in an increasing number of patients. This study explored the use of endothelium-denuded human umbilical veins (HUV) as scaffolds for vascular tissue engineering in a perfusion bioreactor. Vessel diameter ( $1.2\pm 0.4$  mm), wall thickness ( $0.38\pm 0.09$  mm), uniaxial ultimate failure stress ( $8029\pm 1714$  kPa), and burst pressure ( $48.4\pm 20.2$  kPa, range 28.4 - 83.9 kPa) were determined in native samples. The effects of endothelium removal from HUV by enzymatic digestion, hypotonic lysis, and dehydration were assessed. Dehydration did not significantly affect contractile function, tetrazolium dye reduction, mechanical strength, and vessel structure, whereas the other methods failed in at least one of these parameters. Denudation by dehydration retained laminin, fibronectin, collagen, and elastic fibers. Denuded HUV were seeded in a perfusion bioreactor with either allogeneic HUV endothelial cells or with saphenous vein endothelial cells harvested from patients with coronary artery disease. Seeding in a perfusion bioreactor resulted in a confluent monolayer of endothelial cells of both sources as judged by histology and scanning electron microscopy. Seeded cells contained von Willebrand factor and CD31. In conclusion, denuded HUV should be considered an alternative to decellularized blood vessels as the process keeps the smooth muscle layer intact and functional, retains proteins relevant for biomechanical properties and for cell attachment, and provides a suitable scaffold for

1  
2  
3 seeding an autologous and flow resistant endothelium.  
4  
5

6 Keywords: vascular tissue engineering, small caliber graft, endothelium,  
7  
8 biomechanics, human umbilical vein, bioreactor  
9

10  
11  
12  
13  
14  
15  
16  
17  
18  
19  
20  
21  
22  
23  
24  
25  
26  
27  
28  
29  
30  
31  
32  
33  
34  
35  
36  
37  
38  
39  
40  
41  
42  
43  
44  
45  
46  
47  
48  
49  
50  
51  
52  
53  
54  
55  
56  
57  
58  
59  
60

For Peer Review

# 1. Introduction

Coronary artery disease and peripheral vascular disease are common maladies in elderly patients. Both are consequences of atherosclerosis and endothelial dysfunction. Risk factors are partly congenital and partly behavioural, which explains the high incidence of these conditions in western societies. Although symptoms of the diseases like angina pectoris can be treated successfully by pharmaceutical means, many patients eventually require surgical interventions. Coronary artery bypass grafting (CABG) and peripheral revascularization using autologous vessel grafts have turned into routine procedures with good long-term results. However, a considerable number of patients lack suitable autologous vessels due to varicosis, trauma, or prior removal, effectively precluding their optimal treatment. Also, surgical treatment of multi-vessel coronary artery disease usually requires the use of saphenous vein in addition to internal mammary artery. The former has patency rates of about 60% after 10 years due to vein graft disease ([Goldman et al. 2004](#)) and thus may require re-operations with a further limited supply of autologous grafts.

In contrast to the successful use of synthetic polymers like Dacron or ePTFE in the reconstruction of large diameter vessel defects, synthetic small-caliber vessel grafts are still considered inferior to autologous vessels in peripheral revascularization ([Mamode and Scott 1999](#)) and have only rarely been used in CABG ([Hoenig et al. 2006](#)). Synthetic graft failures have been attributed to infections, compliance mismatches, and thrombogenic surfaces ([Bordenave et](#)

1  
2  
3 [al. 2005](#)). Most synthetic polymers suitable as vessel replacements are less  
4  
5 elastic and thus possess a far lower compliance compared to human vessels,  
6  
7 and the lack of an endothelium promotes aggregation and adhesion of platelets.  
8  
9 Consequently, research focused on tissue engineering by combining autologous  
10  
11 cells with biocompatible scaffolds, thus addressing both the mechanical and  
12  
13 thrombogenic issues of small-caliber synthetic grafts. Biocompatible polymers  
14  
15 like collagens and fibrin, biodegradable polymers, and various preparations of  
16  
17 extracellular matrix have been tested for their utility as scaffolds for vascular  
18  
19 tissue engineering [\(Campbell and Campbell 2007\)](#). However, tissue-engineered  
20  
21 vessels often suffer from one or more disadvantages which so far precluded  
22  
23 their clinical use as bypass grafts. Among these are the absence of sufficient  
24  
25 amounts of elastin, insufficient burst strengths, and culture times of up to one  
26  
27 year.  
28  
29

30  
31  
32  
33  
34 Human umbilical cords contain one vein (human umbilical vein, HUV) and  
35  
36 usually two arteries. These vessels are unbranched, have no valves with flaps,  
37  
38 and can be obtained in lengths of up to 50 cm without ethical concerns.  
39  
40

41  
42 Glutaraldehyde-fixed HUV have been used as grafts for peripheral  
43  
44 revascularizations for decades [\(Dardik et al. 2002\)](#). However, these grafts are  
45  
46 entirely acellular, require an external Dacron stent, and merely act as passive  
47  
48 conduits. Due to their lack of a functional endothelium, these grafts have never  
49  
50 been considered for CABG. Decellularized HUV have been suggested as  
51  
52 scaffolds for vascular tissue engineering [\(Daniel et al. 2005\)](#), whereas our group  
53  
54 suggested to use denuded HUV (denHUV) as a semi-finished scaffold, to be  
55  
56  
57  
58  
59  
60

1  
2  
3 completed by the recipient's own endothelial cells ([Hoenicka et al. 2007](#)). This  
4  
5 approach is likely to decrease the time required to assemble and condition the  
6  
7 graft, as the synthetic capabilities of the smooth muscle layer are preserved.  
8  
9 More recently, decellularized human umbilical arteries have been tested as  
10  
11 scaffolds as well ([Gui et al. 2009](#)).  
12  
13

14  
15 We have previously demonstrated that mechanically denuded HUV are suitable  
16  
17 scaffolds for HUVEC seeding under static conditions. To further develop this  
18  
19 material into vessel grafts, the current study explored methods to denude longer  
20  
21 segments of vessels while retaining their mechanical integrity and function, and  
22  
23 to develop seeding procedures in a perfusion system suitable for tissue-  
24  
25 engineering vessel grafts of suitable lengths. Furthermore, the scaffolds were  
26  
27 seeded with human saphenous vein endothelial cells (HSVEC) derived from  
28  
29 CAD patients to demonstrate the feasibility of a recipient-derived endothelium.  
30  
31  
32  
33

## 34 35 **2. Materials and Methods**

### 36 37 **2.1. Harvesting of vascular tissue**

38  
39 Human umbilical cords were procured in the OB/GYN departments of the  
40  
41 participating universities as described previously ([Hoenicka et al. 2008](#)) and  
42  
43 were used for experiments within 40 hours post partum. Written informed  
44  
45 consent was obtained from the expectant mothers before birth commenced.  
46  
47 The cords were stored immediately after birth at 4 °C in Krebs-Henseleit buffer  
48  
49 (KHB; NaCl 118 mM, KCl 4.7 mM, MgSO<sub>4</sub> 1.2 mM, NaH<sub>2</sub>PO<sub>4</sub> 1.2 mM, NaHCO<sub>3</sub>  
50  
51 16.7 mM, dextrose 5.5 mM, CaCl<sub>2</sub> 1.2 mM; chemicals were from Merck,  
52  
53  
54  
55  
56  
57  
58  
59  
60

1  
2  
3 Darmstadt, Germany, or from Sigma, Taufkirchen, Germany, unless noted  
4  
5 otherwise) supplemented with HEPES (25 mM) and penicillin (100 U/ml) /  
6  
7 streptomycin (100 µg/ml, PAA, Pasching, Austria). HUV were dissected free  
8  
9 from connective tissue in a sterile hood. All experiments were in accordance  
10  
11 with the rules of the ethical review boards of the participating universities.  
12  
13  
14

## 15 16 **2.2. Denudation procedures**

17  
18  
19 HUV segments of approx. 8 cm in length were subjected to several procedures  
20  
21 designed to remove the endothelium without affecting the structure and function  
22  
23 of the remainder of the vessel wall. The initial conditions described here were  
24  
25 arrived at empirically, and all further optimizations are reported in the results  
26  
27 section. Segments of the vessels were obtained before and after denudation for  
28  
29 organ bath experiments, tetrazolium dye reduction, and histological analysis. In  
30  
31 all methods, vessels were immersed in cell culture medium during the  
32  
33 procedures to maintain the integrity of the vessel wall as far as possible. Also,  
34  
35 vessels were thoroughly flushed with cell culture medium immediately after the  
36  
37 procedures to remove any debris and to restore a conducive environment.  
38  
39  
40  
41  
42

43  
44 Endothelial cells (EC) were removed enzymatically according to methods  
45  
46 established to harvest EC from umbilical veins ([Jaffe et al. 1973](#)). In brief,  
47  
48 vessels were filled with 0.1% (w/v) collagenase A solution (Roche, Mannheim,  
49  
50 Germany) and incubated at 37 °C in a cell culture incubator. The vessels were  
51  
52 then rinsed thoroughly with M199 (PAA) containing 10% fetal calf serum (FCS,  
53  
54 PAA) to interrupt proteolysis.  
55  
56  
57  
58  
59  
60



1  
2  
3 The second method used hypotonic media to disrupt endothelial cells by  
4 osmotic lysis. The vessels were either slowly perfused with sterile distilled water  
5 at room temperature (for 1 min incubation time), or they were filled with distilled  
6 water and incubated at room temperature (for incubation times longer than  
7  
8  
9  
10  
11  
12  
13 1 min).

14  
15 Denudation method three used a gentle stream of gas to dehydrate EC. This  
16 method is based on earlier reports which investigated the role of endothelium in  
17  
18 small-caliber animal vessels ([Bjorling et al. 1992](#); [Fishman et al. 1975](#)).

19  
20 Carbogen (95% oxygen, 5% carbon dioxide, Linde, Pullach, Germany) flow was  
21  
22 adjusted to 60 ml min<sup>-1</sup> by means of a needle valve. The gas stream was  
23  
24  
25  
26  
27  
28  
29  
30  
31  
32  
33  
34  
35  
36  
37  
38  
39  
40  
41  
42  
43  
44  
45  
46  
47  
48  
49  
50  
51  
52  
53  
54  
55  
56  
57  
58  
59  
60  
passed through a sterile filter into the vessels for 10 min.

### 2.3. Determination of contractile properties

34 Responses to vasoconstrictors were assayed in an organ bath as described  
35  
36 previously ([Hoenicka et al. 2007](#)). In brief, vessel rings of 2 mm segment length  
37  
38 were mounted between stainless steel hooks. The upper hook was attached to  
39  
40 a transducer which allowed to read out isometric forces. The baths were filled  
41  
42 with KH at 37°C and bubbled with a mixture of 5% oxygen and 5% carbon  
43  
44 dioxide (balance nitrogen, Linde). Vessel rings were equilibrated over a period  
45  
46 of approx. 2 hours. Tensions were readjusted repeatedly until a stable baseline  
47  
48  
49  
50  
51  
52  
53  
54  
55  
56  
57  
58  
59  
60  
was established at approx. 20 mN. Then the response to 150 mM KCl was  
read. After allowing the rings to return to the baseline, dose-response curves to  
5-hydroxytryptamine (5-HT, Sigma) were constructed. Four to eight rings per

1  
2  
3 sample were analyzed.  
4  
5

## 6 7 **2.4. Determination of tetrazolium dye reduction** 8

9  
10 Cells and tissues reduce tetrazolium dyes to chromophores whose  
11 concentrations are proportional to the reductive capacities. The enzymatic  
12 conversion of the chromogenic substrate 3-(4,5-dimethylthiazol-2-yl)-5-(3-  
13 carboxymethoxyphenyl)-2-(4-sulfophenyl)-2H-tetrazolium (MTS, Promega,  
14 Madison, WI, USA) on the luminal face of longitudinally opened vessels was  
15 determined as described previously ([Hoenicka et al. 2007](#)), using three to five  
16 wells per sample.  
17  
18  
19  
20  
21  
22  
23  
24  
25

## 26 27 **2.5. Determination of tensile strength** 28

29  
30 Mechanical properties of vessel segments were determined in a tensile testing  
31 rig (Inspekt Desk 50, Hegewald & Peschke, Nossen, Germany) equipped with a  
32 20 N load cell (KAP-S, Peekel Instruments, Rotterdam, Netherlands). Vessel  
33 rings of 3 mm segment length were mounted between two cylindrical supports  
34 and strained uniaxially until they failed, using a constant speed of 10 mm min<sup>-1</sup>.  
35 Force and displacement data were used to construct stress-strain relationships  
36 and to determine ultimate failure stresses. Four to five rings were analyzed per  
37 sample.  
38  
39  
40  
41  
42  
43  
44  
45  
46  
47  
48

49  
50 Representative vessel segments (n=15 with 4 sections per vessel) were used to  
51 determine internal diameters and wall thicknesses at physiological pressure  
52 near term. The segments were mounted on glass tubes, filled with phosphate-  
53 buffered formalin (4%), and sealed on on the opposite end. A hydrostatic  
54  
55  
56  
57  
58  
59  
60

1  
2  
3 pressure equivalent to 15 mm Hg was applied for 10 min after which the  
4  
5 samples were transferred to formalin and fixed overnight. Samples were then  
6  
7 embedded in paraffin and stained using a standard H&E protocol. The area of  
8  
9 the lumen, and the area of the smooth muscle layer were determined in each  
10  
11 sample morphometrically. Idealized circular rings were computed from these  
12  
13 data and provided internal diameters, median diameters, and wall thicknesses  
14  
15 for further calculations.  
16  
17  
18

## 20 21 **2.6. Determination of burst pressure**

22  
23 Burst pressures of vessels were measured in a custom built instrument (Fig. 1).  
24  
25 A 10 ml syringe was driven by a computer-controlled stepper motor and  
26  
27 delivered a 5% (w/v) solution of methylcellulose in phosphate-buffered saline at  
28  
29 a flow rate of 3.0 ml min<sup>-1</sup>. Samples of 6 cm in length were mounted on glass  
30  
31 tubes of 3 mm outer diameter. One glass tube was equipped with a stopcock,  
32  
33 the other was attached to the syringe using silicone tubing. Luminal pressure  
34  
35 between syringe and sample was read out by a pressure transducer with a  
36  
37 precision of 0.1% (Wagner Meß- und Regeltechnik, Offenbach, Germany).  
38  
39 Samples were monitored by two orthogonally mounted USB cameras (Webcam  
40  
41 9000, Logitech, Morges, Switzerland). Volume, pressure, and video data were  
42  
43 saved in a synchronized fashion which facilitated correlating the sudden drop of  
44  
45 luminal pressure with visual clues of bursting. As the measured burst pressures  
46  
47 are likely to depend on the quality of vessel dissection (see discussion),  
48  
49 samples were prepared independently by two skilled persons. One to four  
50  
51 segments per subject were measured.  
52  
53  
54  
55  
56  
57  
58  
59  
60

## 2.7. Cell culture

HUVEC were isolated enzymatically from human umbilical veins ([Jaffe et al. 1973](#)) and further cultured in M199 supplemented with 10% FCS (both from PAA) and endothelial cell culture supplement (Promocell, Heidelberg, Germany). HSVEC were prepared enzymatically from human saphenous veins and cultured in the same medium except that 20% serum were used. Both cell types were trypsinized (trypsin-EDTA, Sigma) at confluence and expanded to sufficient cell numbers. Cells of passages 1 and 2 for HUVEC and HSVEC, respectively, were harvested for seeding experiments. These cells were incubated with Calcein AM ( $1 \mu\text{g ml}^{-1}$ , Molecular Probes, Eugene, OR, USA) for 60 min at  $37^\circ\text{C}$  prior to seeding to facilitate easy identification of seeded cells in histological sections.

## 2.8. Perfusion System

Details of the perfusion system have been published previously ([Hoenicka et al. 2010](#)). In brief, mock circulations were set up consisting of media reservoirs, membrane oxygenators, separate peristaltic pumps for the perfusion and superfusion loops, compliance chambers, and vessel chambers. The oxygenators and the vessel chambers were kept at  $37 \pm 0.05^\circ\text{C}$ . Each circulation was filled with M199 supplemented with 20% FCS at  $37^\circ\text{C}$ . The oxygenators were perfused with a mixture of 20% oxygen and 5% carbon dioxide (balance nitrogen, Linde). Oxygen and carbon dioxide partial pressures as well as pH were monitored with a blood gas analyzer (ABL 800, Radiometer, Willich,

Germany). Vessel chambers were connected to computer-controlled stepper motors via timing belts to provide continuous or intermittent rotation during seeding procedures. Rotational speeds were adjustable between 0.06 and 60 rpm. Intermittent rotation included breaks of adjustable length after each 90° turn, providing some time of static incubation for cells to settle and adhere.

## **2.9. Seeding procedure**

After mounting the scaffolds in the vessel chambers, perfusion and superfusion pumps were set to 20 ml/min and 40 ml/min, respectively. Scaffolds were equilibrated for 1 h under flow (Fig. 2). Prior to adding the cells, the perfusion was shut off, whereas the superfusion continued to run throughout the entire seeding procedure to maintain nutrient and oxygen delivery to the vessel walls. Cell suspensions were injected through ports in the perfusion loop at a concentration of approx.  $5 \times 10^6$  cells  $\text{ml}^{-1}$ . Immediately after injecting the cells, automated rotation was started. After finishing the adhesion step (60 min), rotation was stopped, and the perfusion was turned on briefly to remove non-adhering cells and to replenish fresh medium inside the vessels. After an additional 60 min of static incubation, vessels were perfused continuously until the experiment was terminated. The constructs were then fixed in situ by slowly infusing phosphate-buffered formalin (4%). One half of each sample was used for histological analysis, the other half was further treated in phosphate-buffered paraformaldehyde (2%) supplemented with 2.5% glutardialdehyde for scanning electron microscopy (SEM).

## 2.10. Histology and immunohistochemistry

Formaldehyde-fixed samples were embedded in paraffin. Thin sections were prepared in a microtome and mounted on glass slides. Fluorescently labelled cells were visualized under UV illumination using appropriate band-pass filters on a Leica DMRBE microscope (Leitz, Wetzlar, Germany). Histological staining was done using standard protocols. General morphology was analyzed in hematoxylin and eosin (Chroma, Münster, Germany) stained slides. Elastic laminae and collagen were visualized with resorcin-fuchsin (Chroma) and Sirius red (Sigma), respectively. Specific antibodies were used to label laminin (clone LAM-89, monoclonal from mouse, Sigma), fibronectin (A0245, polyclonal from rabbit, Dako, Glostrup, Denmark), CD31 (clone JC70A, monoclonal from mouse, Dako), von Willebrand factor (A0082, polyclonal from rabbit, Dako), and  $\alpha$ -smooth muscle cell actin (clone 1A4, monoclonal from mouse, Sigma). Bound antibodies were visualized using biotinylated secondary antibodies (donkey anti rabbit and donkey anti mouse IgG [H+L], Jackson ImmunoResearch, Suffolk, UK) and the Vectastain Elite ABC kit (Vector, Burlingame, CA, USA) according to the manufacturer's protocol. Diaminobenzidine (Sigma) was used as chromogenic substrate.

## 2.11. Scanning Electron Microscopy

Formalin/glutaraldehyde-fixed vessel samples were dehydrated and sputtered with gold using standard protocols. Samples were analyzed in a Quanta-400F scanning electron microscope (FEI, Hillsboro, OR, USA) using an accelerating

voltage of 10 kV.

## 2.12. Data Analysis and Statistics

Numerical data are reported as means±standard deviation. The number of repeats  $n$  refers to the number of subjects. Treatments were compared using analysis of variance (ANOVA) followed by Holm-Sidak post-tests. Dose-response curves were analyzed by fitting a Hill function, which allowed to compute maximum responses and half maximal effective concentrations ( $EC_{50}$ ). Dose-response curves were compared by two-way ANOVA. Differences were assumed to be statistically significant if the error probability  $p$  was less than 0.05.

The data obtained from the tensile testing experiments were used to calculate ultimate failure stresses and extrapolated burst pressures. The undeformed cross section areas  $S_0$  of the rings were calculated from the wall thickness  $t_0$  and the segment length  $l_0$ :

$$S_0 = 2 \times t_0 \times l_0 \quad (1)$$

The engineering (1. Piola-Kirchhoff) stress is calculated from the ultimate failure force  $F$  according to (2):

$$\sigma_{uPK} = \frac{F}{S_0} \quad (2)$$

The true (Cauchy) stress can be calculated from this quantity by multiplying it with the ultimate stretch ratio  $\lambda_t$  (3):

$$\sigma_{uC} = \sigma_{uPK} \times \lambda_t \quad (3)$$

To compute the extrapolated burst pressures, the deformed radius  $R$  is calculated from the undeformed radius  $R_0$  and the stretch ratio  $\lambda$  according to

(4):

$$R = \lambda_t \times R_0 \quad (4)$$

The other deformed dimensions of the ring can be calculated from the incompressibility condition in the form  $J = \lambda_t \times \lambda_r \times \lambda_a = 1$ , where  $t$ ,  $r$ , and  $a$  denote the circumferential, radial, and axial dimensions, respectively, of the rings in a cylindric coordinate system. As an initial approximation it was assumed that the material is isotropic. Then it holds  $\lambda_r = \lambda_a$ . Therefore,

$$\lambda_r = \sqrt{\frac{1}{\lambda_t}} \quad (5)$$

The deformed specimen thicknesses  $t$  and lengths  $l$  can be computed from these stretch ratios and the initial dimensions  $t_0$  and  $l_0$ . The resulting extrapolated burst pressure is then calculated using the Laplace law according to (6):

$$P_{burst} = \frac{\sigma_c \times t}{R} \quad (6)$$

The internal diameter  $d_i$  of the vessels during burst pressure measurements were computed according to (7) from the average outer diameter  $d_o$  along the entire sample using the histologically determined wall thickness at 15 mm Hg, assuming that the cross-sectional wall area  $A$  remains constant due to incompressibility of the wall.



$$d_i = 2 \times \sqrt{\frac{(0.5d_o)^2 \pi - A}{\pi}} \quad (7)$$

### 3. Results

#### 3.1. Endothelium removal

If denuded HUV are to be seeded with autologous endothelial cells, the existing endothelium has to be removed entirely, not just inactivated. Starting from initial conditions taken from the literature, if available, all three denudation methods were optimized to effect complete removal of endothelial cells from the luminal surface of HUV as judged by histology. At least five vessels were evaluated per condition in this initial screening. Fig. 3A shows a native control with intact endothelial and smooth muscle layers. Collagenase treatments of 10, 20, and 30 min were tested. Essentially all EC were removed after 20 min (Fig. 3B). However, in many cases the structural integrity of the vessel wall was visibly affected and sometimes the smooth muscle layer appeared spongiform. Denudation by a gas stream was tested at 5, 10, and 20 min. Complete EC removal was accomplished after 10 min (Fig. 3C). Fig. 3D-F shows a time course (1, 3, and 5 min) of hypotonic treatment with distilled water. Incubation times of 5 min were required to destroy and remove virtually all endothelial cells.

#### 3.2. Vessel dimensions and mechanical properties

Internal diameters of HUV under moderate pressure (15 mm Hg) were

1  
2  
3 determined as  $1.2\pm 0.4$  mm. Wall thicknesses amounted to  $0.38\pm 0.09$  mm. In  
4  
5 order to assess the influence of denudation treatments on the mechanical  
6  
7 stability of vessels, HUV were cut into four segments. One served as native  
8  
9 control, whereas the others were subjected to the optimized denudation  
10  
11 methods. Force-distension relationships of these specimens were determined  
12  
13 (Fig. 4 A). The resulting stress and strain data were used in conjunction with the  
14  
15 morphometric data to compute theoretical burst pressures. Denudation by  
16  
17 dehydration and denudation by osmotic lysis did not affect tensile strength,  
18  
19 whereas collagenase treatment significantly reduced the strength of the vessel  
20  
21 rings (RM ANOVA,  $p=0.007$ ,  $n=5$ , Table 1). All extrapolated burst pressures  
22  
23 exceeded 1200 mm Hg.  
24  
25  
26  
27  
28

29  
30 Volume-pressure relationships and burst pressures of native vessel segments  
31  
32 were determined experimentally ( $n=8$ ). A representative burst experiment is  
33  
34 shown in Fig. 4 B. The burst pressures were calculated as  $362.7\pm 151.7$  mm Hg  
35  
36 /  $48.4\pm 20.2$  kPa (range 213.3 - 629.3 mm Hg / 28.4 - 83.9 kPa).  
37  
38  
39

### 40 **3.3. Influence of denudation on contractile function**

41  
42  
43 The response to vasoconstrictors is a key feature and a sensitive marker of  
44  
45 vessel wall integrity. Receptor-independent vasoconstriction was induced by  
46  
47 adding 150 mM KCl to the baths. Responses of gas-denuded HUV did not differ  
48  
49 from native controls. However, HUV treated by collagenase or by osmotic lysis  
50  
51 showed significantly decreased contractions to KCl (RM ANOVA,  $p=0.005$ ,  $n=7$ ,  
52  
53 Table 2).  
54  
55  
56  
57  
58  
59  
60

1  
2  
3  
4  
5  
6  
7  
8  
9  
10  
11  
12  
13  
14  
15  
16  
17  
18  
19  
20  
21  
22  
23  
24  
25  
26  
27  
28  
29  
30  
31  
32  
33  
34  
35  
36  
37  
38  
39  
40  
41  
42  
43  
44  
45  
46  
47  
48  
49  
50  
51  
52  
53  
54  
55  
56  
57  
58  
59  
60

5-HT is one of the most potent receptor-mediated vasoconstrictors in HUV\_ ([Hoenicka et al. 2007](#)). Gas denudation did not affect 5-HT dose-response curves compared to native controls, whereas both collagenase treatment and osmotic lysis attenuated responses to this compound (RM ANOVA,  $p=0.001$ ,  $n=7$ , Fig. 5).  $EC_{50}$  values of collagenase-treated HUV were significantly higher compared to native controls and to gas-denuded vessels (RM ANOVA,  $p=0.006$ ,  $n=7$ , Table 2).

### 3.4. Influence of denudation on reductive capacities

Tetrazolium dye reduction is a measure of the reductive capacities of cells and tissues and as such a useful marker to assess effects of treatments on energy metabolism. Denudation did not affect reductive capacities after any of the treatments, indicating that the contribution of the endothelium to dye reduction was small and that the metabolism of the remainder of the vessel wall was left intact (RM ANOVA,  $p=0.542$ ,  $n=6$ , Table 2).

### 3.5. Histological Analysis of native and denuded HUV

The structures and compositions of native and denuded vessel walls were analyzed by histochemistry and immunohistochemistry (Fig. 6). H&E staining revealed the gross structure of the vessels including the endothelium. Native vessel sections contained an intact endothelial layer as well as a strong pink staining of the cytoplasm and a less intense staining of extracellular matrix. Denuded vessels were devoid of endothelial cells as desired. Collagenase treatment mostly affected the staining of the matrix, but it also caused a weaker

1  
2  
3 intracellular staining on the luminal side. There were no visible changes in the  
4  
5 smooth muscle and subendothelial layer of gas-denuded and water/NaCl-  
6  
7 denuded vessels compared to the native controls. The  $\alpha$ -smooth muscle actin  
8  
9 antibody stained the entire smooth muscle layer homogenously. As expected,  
10  
11 the stain was present only inside the cells. Denuded vessels did not stain  
12  
13 differently from native vessels. Superficial differences in the staining intensity  
14  
15 are due to different densities and orientations of individual smooth muscle cells.  
16  
17  
18 Extracellular matrix proteins are important for the remodelling and cell adhesion  
19  
20 properties of scaffolds. Fibronectin is commonly associated with extracellular  
21  
22 matrix in vessel walls. Native HUV showed an extracellular staining throughout  
23  
24 the entire smooth muscle layer. There was a very intense staining in the  
25  
26 subendothelial layer. Collagenase treatment caused a decrease of the staining  
27  
28 intensity on the luminal side of the smooth muscle layer. There was no staining  
29  
30 in the subendothelial layer. Denudation by dehydration or by osmotic lysis did  
31  
32 not alter the fibronectin staining properties compared to the native controls.  
33  
34 Laminin was also present throughout the smooth muscle layer. However, in  
35  
36 contrast to fibronectin there was no intense staining of the subendothelial layer.  
37  
38 Denudation by dehydration or by osmotic lysis did not affect laminin staining,  
39  
40 whereas collagenase treatment caused a slightly weaker staining on the luminal  
41  
42 side compared to native controls. Resorcin was used to visualize elastic fibers.  
43  
44 Native vessels showed an intense staining of the subendothelial layer, with  
45  
46 usually 2-4 slightly less intense layers underneath. In most samples, the entire  
47  
48 smooth muscle layer contained weakly stained strands of elastic fibers.  
49  
50  
51  
52  
53  
54  
55  
56  
57  
58  
59  
60

1  
2  
3  
4  
5  
6  
7  
8  
9  
10  
11  
12  
13  
14  
15  
16  
17  
18  
19  
20  
21  
22  
23  
24  
25  
26  
27  
28  
29  
30  
31  
32  
33  
34  
35  
36  
37  
38  
39  
40  
41  
42  
43  
44  
45  
46  
47  
48  
49  
50  
51  
52  
53  
54  
55  
56  
57  
58  
59  
60

Collagenase treatment strongly affected the staining of the subendothelial layer, leaving only a minor amount of the resorcin-stainable material in the vessel. In contrast, denudation by dehydration and by osmotic lysis did not affect elastic fibers. Finally, sirius red was used to stain collagen, a major component of the extracellular matrix. The entire smooth muscle layer was stained intensely red, with a weakly yellow stain inside the cells. As expected, collagenase treatment affected sirius red staining on the luminal side, whereas there was no such effect after applying the other denudation methods.

### **3.6. Seeding of denuded HUV**

Based on the results described above, all vessels used in seeding experiments were denuded by dehydration. Translation of a static seeding model using longitudinally opened vessels to a perfusion system using tubular vessels necessitated the development of rotational patterns which optimized both homogenous distribution of the seeded cells and complete coverage.

Optimization of cell distribution was done using HUVEC labelled with Calcein AM with at least 3 independent experiments per condition. First, continuous rotation was compared to intermittent rotation, using a total seeding time of 60 min. Rotational speeds were varied between 0.12 and 0.5 rpm. However, histological analysis revealed that none of the tested rotational speeds resulted in reasonable amounts of adherent cells (not shown). Second, intermittent rotation was optimized. This required the adjustment of two parameters, rotational speed and length of the static phases. Rotational speeds of 0.25, 0.5, and 1 rpm and static phases of 1 min to 5 min were evaluated. The results were

1  
2  
3 largely independent of rotational speed but sensitive to the duration of static  
4  
5 phases. 5 min tended to create alternating longitudinal strips of seeded and  
6  
7 cell-free areas, whereas 1 min reduced the overall number of adhering cells.  
8  
9 Based on these observations, rotation at 0.5 rpm interrupted by 3 min static  
10  
11 phases were used in all subsequent seeding experiments.  
12  
13  
14

15  
16 The initial endothelial cell coverage was supposed to be as complete as  
17  
18 possible in order to avoid cell-free patches that might act as starting points of  
19  
20 endothelium loss once shear forces were applied. Critical factors affecting  
21  
22 coverage are seeding cell density and total incubation time. Based on our  
23  
24 previous experience with static seeding models, cell suspensions ranging from  
25  
26 5E5 to 1E7 cells/ml were applied for one hour. Assuming an average diameter  
27  
28 of the vessels of 3 mm during perfusion, these suspensions resulted in seeding  
29  
30 densities of 6.6E4 to 1.3E6 cells per cm<sup>2</sup>. In general, the lowest concentrations  
31  
32 did not provide sufficient coverage, whereas the highest concentrations tended  
33  
34 to acidify the medium in the lumen of the vessels visibly. Therefore  
35  
36 concentrations of approx. 5E6 cells were used in all further experiments.  
37  
38  
39

40  
41 Extending the incubation time beyond one hour did not further increase  
42  
43 endothelial coverage. In order to obtain best possible results, the vessels were  
44  
45 perfused briefly after the first hour of incubation, and a second batch of cells  
46  
47 was injected, followed by another hour of intermittent rotation.  
48  
49

50  
51 The results obtained with a protocol based on the above mentioned  
52  
53 optimizations are shown in figures 7 and 8. Both images are representative for 5  
54  
55 independent experiments per condition. All vessels were perfused for 24 h after  
56  
57  
58  
59  
60

1  
2  
3 seeding at 20 ml/min. Figure 7 demonstrates that there were no differences in  
4 the appearance of cross sections of denuded HUV seeded with HUVEC and  
5 HSVEC. Both formed continuous monolayers. Figure 8 Panel A depicts the  
6 surface of native HUV as seen by SEM. Endothelial cells were densely packed  
7 and fairly small. After denuding HUV, the basal membrane on top of the smooth  
8 muscle layer was visible (Panel B). Seeding with HUVEC resulted in a  
9 completely covered surface. The cells appeared flattened, each one covering a  
10 larger area compared to native EC (Panel C). Seeding with HSVEC resulted in  
11 a similar endothelial coverage (Panel D), although the cells appeared slightly  
12 smaller compared to HUVEC.  
13  
14  
15  
16  
17  
18  
19  
20  
21  
22  
23  
24  
25  
26

27 The identity of seeded endothelial cells was verified using two markers. CD31 is  
28 a surface protein expressed on endothelial cells, whereas von Willebrand factor  
29 (vWF) is a protein synthesized in and secreted from endothelial cells. Cross  
30 sections of gas-denuded HUV and of EC-seeded HUV were stained with  
31 specific antibodies for each marker. Fig. 9 shows that the seeded cells express  
32 CD31 on their surfaces. vWF is also present, although a considerable level of  
33 staining is found in the subendothelial layer and was present before seeding.  
34  
35  
36  
37  
38  
39  
40  
41  
42  
43  
44

## 4. Discussion

45  
46  
47  
48  
49 The necessity of artificial vessel grafts has long been recognized, either as an  
50 alternative to harvesting autologous vessels, or as a substitute if suitable  
51 autologous vessels are not available. In the past decades, a variety of scaffolds  
52 for vascular tissue engineering have been evaluated with mixed success.  
53  
54  
55  
56  
57  
58  
59  
60

1  
2  
3 Synthetic polymers often do not achieve suitable mechanical and antithrombotic  
4  
5 properties. Therefore, tubular organs of animal or human origin have attracted  
6  
7 attention because of their wall structures, mechanical properties, and lack of  
8  
9 foreign body reactions after suitable treatments. Decellularized blood vessels  
10  
11 (reviewed in [\(Hoenig et al. 2005\)](#)) and ureters [\(Narita et al. 2008; Derham et al.](#)  
12  
13 [2008; Clarke et al. 2001\)](#) of various species have been investigated for their  
14  
15 utility as biological conduits, requiring recellularization in vivo, or as scaffolds for  
16  
17 vascular tissue engineering. Recellularization can be readily achieved in various  
18  
19 species, including dog and sheep, which usually also manage to grow a  
20  
21 confluent autologous endothelium on grafts. These results are enticing, but  
22  
23 usually reflect a transanastomotic growth of endothelial cells on the often short  
24  
25 grafts. In humans, this type of endothelial growth rarely exceeds 2 cm in length  
26  
27 and is clearly insufficient for both coronary and peripheral bypass grafts which  
28  
29 usually require ten times this length [\(Zilla et al. 2007\)](#). Endothelialization is of  
30  
31 utmost importance for graft patency as it suppresses thrombogenesis and graft  
32  
33 rejection. Therefore, tissue engineering is currently the most promising  
34  
35 approach, as it allows to grow an autologous endothelium from patient-derived  
36  
37 endothelial cells in vitro.

38  
39 Human umbilical vessels have been evaluated for their utility as bypass grafts  
40  
41 previously. HUV is an unbranched vessel which can be harvested in lengths  
42  
43 suitable for one or two coronary bypasses. The diameter of vessel cross  
44  
45 sections was determined in the present study as approx. 1.2 mm under  
46  
47 moderate pressure (15 mm Hg). This was less than the value of 2.4 mm  
48  
49  
50  
51  
52  
53  
54  
55  
56  
57  
58  
59  
60



1  
2  
3 reported for term pregnancies in a recent study ([Li et al. 2008](#)). The lower  
4 values may be attributed to a gentler method of sample preparation in the  
5 present study (dissection vs. "stripping"). It should also be noted that the  
6 diameter is up to 5 mm in utero as measured by ultrasound ([Rigano et al.](#)  
7 [2008](#)), which is also roughly the diameter of the umbilical vein-based UVg graft\_  
8 ([Dardik et al. 2002](#)). Our burst pressure measurements indicated that umbilical  
9 veins distend to almost this diameter under arterial pressure. Therefore HUV  
10 are properly sized for small-diameter bypass grafts.

11  
12  
13 HUV have been tanned and wrapped in dacron sheets to use them as  
14 peripheral bypass grafts with good results ([Dardik et al. 2002](#)). However, these  
15 grafts have never been considered for coronary bypass grafting. Using  
16 decellularized umbilical vessels was suggested both for veins ([Daniel et al.](#)  
17 [2005](#)) and for arteries ([Gui et al. 2009](#)). Unfortunately, procedures based on  
18 decellularized tissues face several problems. First, the chemicals or enzymes  
19 used to remove the cells may require tedious post-processing to remove or  
20 inactivate them. Second, the generation of a layered wall structure is difficult to  
21 achieve in vivo, as there is usually only minor cell ingrowth from the surfaces\_  
22 ([Gui et al. 2009](#)). Third, the time to engineer a fully repopulated and  
23 endothelialized graft in vitro is usually too long for on-demand production. We  
24 have suggested to overcome these limitations by using endothelium-denuded  
25 HUV and seed these with autologous cells derived from the recipient ([Hoenicka](#)  
26 [et al. 2007](#)). This way, there is a layered wall structure with vital cells from the  
27 start, and matrix synthesis by smooth muscle cells present in denuded vessel  
28  
29  
30  
31  
32  
33  
34  
35  
36  
37  
38  
39  
40  
41  
42  
43  
44  
45  
46  
47  
48  
49  
50  
51  
52  
53  
54  
55  
56  
57  
58  
59  
60

1  
2  
3 walls is likely to reduce the time of the tissue-engineering procedure  
4  
5 considerably. Also, it was shown previously that allogeneic vessel  
6  
7 transplantations succeed without immunosuppression if the denuded vessels  
8  
9 are seeded with autologous endothelial cells before implantation ([Lamm et al.](#)  
10  
11 [2001](#)).

12  
13  
14  
15 In our previous study, patches of HUV were denuded mechanically and seeded  
16  
17 under static conditions, providing a first proof of concept that a confluent  
18  
19 allogeneic endothelium can be generated on this type of scaffold. The present  
20  
21 study attempted to create endothelium-seeded grafts under perfusion  
22  
23 conditions. Therefore methods to denude longer segments of HUV had to be  
24  
25 developed. Based on reports in the literature and on our own preliminary  
26  
27 experiments, three methods were evaluated in detail with respect to their  
28  
29 simplicity, reproducibility, and effect on vessel wall structure and function. The  
30  
31 first method is a slight modification of a well-established procedure to harvest  
32  
33 endothelial cells from umbilical veins ([Jaffe et al. 1973](#)). Usually the incubation  
34  
35 time is optimized to ensure purity of the harvested cells at the expense of yield.  
36  
37 In order to create an endothelium-denuded scaffold, the incubation time had to  
38  
39 be optimized to ensure complete removal of endothelial cells. This required  
40  
41 longer incubations (20 min vs. 10 min for cell harvesting). However, this method  
42  
43 had a noticeable impact on the structure of the vessel as well as on its function.  
44  
45 Although there was no decrease in reductive capacity, indicating an unaltered  
46  
47 energy metabolism, contractions induced by KCl or by 5-HT were significantly  
48  
49 weaker. The failure stresses were significantly reduced as well. Histology  
50  
51  
52  
53  
54  
55  
56  
57  
58  
59  
60

1  
2  
3 revealed that smooth muscle actin was largely unaffected, whereas collagen,  
4  
5 elastin, fibronectin, and to a smaller degree also laminin stained weaker on the  
6  
7 luminal side. This is easily explained by the loss of anchoring sites due to the  
8  
9 digestion of parts of the collagen framework. Many vessels also showed  
10  
11 structural defects as a consequence of collagen loss. These resulted in  
12  
13 significantly lower failure stresses compared to the native controls.  
14  
15

16  
17 Hypotonic media have been used to lyse cells in various contexts ([Kong et al.](#)  
18  
19 [2008; Crowston et al. 2004](#)). Preliminary experiments have shown that this  
20  
21 method is also suitable to lyse cells on the luminal face of blood vessels if the  
22  
23 vessels are flushed or filled with distilled water. Time courses demonstrated that  
24  
25 it took 5 min to completely destroy and remove endothelial cells. However,  
26  
27 contractile responses to KCl and 5-HT were attenuated after incubations as  
28  
29 short as 3 min, and were significantly lower after 5 min incubations. Histological  
30  
31 evaluation confirmed that this treatment specifically removed endothelial cells  
32  
33 without affecting any of the investigated components. Failure stresses were not  
34  
35 affected.  
36  
37

38  
39 Dehydration of endothelial cells by a stream of gas has originally been used to  
40  
41 investigate the role of endothelium in microvessels too small for mechanical  
42  
43 denudation ([Bjorling et al. 1992; Fishman et al. 1975](#)). However, we found this  
44  
45 method useful for denuding HUV as well. The residence time, i.e. the time it  
46  
47 took to replace the gas volume in our samples, can be estimated as 0.1 s. It  
48  
49 seems quite unlikely that the gas gets saturated with humidity in this short  
50  
51 amount of time. Therefore the method is likely to work also for segments longer  
52  
53  
54  
55  
56  
57  
58  
59  
60

1  
2  
3 than those used in this study. At the flow rate and incubation time which were  
4  
5 found to remove the endothelium reproducibly, none of the functional and  
6  
7 mechanical parameters was affected. Histological analysis also confirmed that  
8  
9 the treatment solely affected the endothelium.  
10  
11

12  
13 Two key results from the histological analysis should be pointed out: first, while  
14  
15 HUV lack an external elastic lamina, they contain copious amounts of elastin in  
16  
17 the subendothelial layer as well as throughout the smooth muscle layer, which  
18  
19 positively affects their elastic properties. Second, denudation retains proteins,  
20  
21 especially fibronectin and laminin, which are considered important for  
22  
23 endothelial cell attachment and growth, whereas decellularized vessels usually  
24  
25 require precoating with one of these proteins to facilitate endothelial cell  
26  
27 adhesion [\(Gui et al. 2009\)](#).  
28  
29  
30  
31

32  
33 The mechanical properties of HUV were investigated by determining the stress-  
34  
35 strain relationships of HUV rings in an uniaxial tensile testing rig and by  
36  
37 measuring the burst pressure of HUV segments directly. The stress-strain  
38  
39 curves of HUV displayed a biphasic behaviour which is commonly found in  
40  
41 blood vessels. This was not altered by any of the denudation procedures. The  
42  
43 corresponding pressure-volume relationships of intact vessels display a slightly  
44  
45 different behaviour which can be best described as triphasic. A fairly steep initial  
46  
47 phase was followed by a rather flat intermediate phase at physiological arterial  
48  
49 pressures. Additional pressure resulted in a second steep phase until the vessel  
50  
51 failed. The mechanism and the structural base of this behaviour require further  
52  
53 biomechanical analyses which are currently under way. The burst pressures  
54  
55  
56  
57  
58  
59  
60

1  
2  
3 varied between 213.3 and 629.3 mm Hg. This may indicate a problem of  
4  
5 dissecting the vessels cleanly without injuring the vessel wall. This also resulted  
6  
7 in a marked deviation of the burst pressures extrapolated from the stress-strain  
8  
9 curves and the experimentally determined values. The latter were found to be  
10  
11 considerably lower. Several factors contribute to this deviation. First, vessels  
12  
13 measured in the burst pressure apparatus fail at their weakest point by design,  
14  
15 whereas the failure stresses of the replicates of each sample in the tensile  
16  
17 testing experiments were averaged. Second, experimental determination of  
18  
19 burst pressures exerted biaxial stress whereas tensile testing was uniaxial.  
20  
21 Biaxial ultimate stresses are substantially lower than uniaxial ones even in  
22  
23 isotropic elastomers, and the stress-strain curves differ also in these materials.  
24  
25 Moreover, the data suggest that HUV are less resistant to axial stress compared  
26  
27 to circumferential stress and thus appear to be anisotropic. When comparing  
28  
29 these burst pressures with those of autologous bypass vessels or artificial  
30  
31 vessel grafts, it should be taken into consideration that the parameters of vessel  
32  
33 conditioning in a perfusion bioreactor, which was not done in this initial study,  
34  
35 are usually optimized to increase extracellular matrix formation and thus to  
36  
37 increase mechanical stability.  
38  
39  
40  
41  
42  
43  
44  
45

46 With these results at hand, dehydration of the endothelium by a stream of gas  
47  
48 appeared to be the most appropriate technique to denude HUV and was used  
49  
50 in all subsequent seeding experiments. Most importantly, neither contractile  
51  
52 responses as an indicator of general smooth muscle cell function nor  
53  
54 tetrazolium dye reduction were affected by the procedure. Therefore it is  
55  
56  
57  
58  
59  
60

1  
2  
3 reasonable to expect that biosynthetic functions remain intact as well and allow  
4  
5 vessel wall remodeling during a conditioning step.  
6  
7

8  
9 The seeding experiments in this study had two main goals: first, to show that  
10  
11 seeding denuded HUV works in a perfusion bioreactor. Second, to show that  
12  
13 HSVEC from CAD patients, in addition to the commonly used HUVEC, are  
14  
15 suitable for regenerating a confluent endothelium on denuded HUV. The  
16  
17 seeding concentration of  $5E6$  cells  $ml^{-1}$  resulted in a seeding density of approx.  
18  
19  $1.5E6$  cells  $cm^{-2}$  and was arrived at empirically. This value is considerably  
20  
21 higher compared to the one applied during static seeding ( $3E4$  cells  $cm^{-2}$ ) in our  
22  
23 previous study ([Hoenicka et al. 2007](#)). Apparently the curvature of the scaffold  
24  
25 makes it more difficult for cells to attach, requiring higher local concentrations to  
26  
27 succeed. The perfusion system used in the present study allowed to employ  
28  
29 continuous or intermittent rotation of the denuded vessel samples after applying  
30  
31 the endothelial cells. Interestingly, continuous rotation even at extremely slow  
32  
33 angular velocities did not allow endothelial cells to attach to the denuded  
34  
35 surface in reasonable numbers. EC seem to require a minimum of one to three  
36  
37 minutes of entirely static conditions to attach successfully. On the other hand,  
38  
39 too long a static phase during intermittent rotation caused longitudinal "strips" of  
40  
41 endothelium to form, as the cells apparently move towards the lowest point in  
42  
43 the curvature of the scaffold fairly rapidly due to gravity. This was avoided by  
44  
45 limiting the static phases to three minutes, and by repeating the seeding step  
46  
47 with a second batch of cells.  
48  
49  
50  
51  
52  
53  
54  
55

56 Our experiments also showed that there were only minor differences between  
57  
58  
59  
60

1  
2  
3 HUVEC-seeded and HSVEC-seeded scaffolds based on histology,  
4 immunohistology, and scanning electron microscopy. Both types of cells were  
5  
6 equally able to restore a confluent monolayer of cells. However, regenerated  
7  
8 endothelia with either cell type differed greatly in appearance from their native  
9  
10 counterparts. Native endothelial cells usually appeared tightly packed in a  
11  
12 palisade-like fashion in vessel cross sections. Seeded cells appeared flattened  
13  
14 instead. Also, native endothelium consisted of fairly small and slightly irregular  
15  
16 cells when viewed en face under a scanning electron microscope. In contrast,  
17  
18 seeding resulted in homogenous layers of fairly large cells. At this preliminary  
19  
20 stage it is yet unclear whether this morphology changes if the constructs are  
21  
22 conditioned with elevated shear forces or luminal pressure.  
23  
24  
25  
26  
27  
28  
29  
30

## 31 **5. Conclusions**

32  
33  
34 This study explored the utility of endothelium-denuded HUV for vascular tissue  
35  
36 engineering. Longer segments of HUV can be effectively endothelium-denuded  
37  
38 by passing a stream of carbogen through the lumen. As both contractile function  
39  
40 and reductive capacities are unaltered and proteins relevant for endothelial cell  
41  
42 attachment are unaffected by this procedure, the procedure appears to be an  
43  
44 interesting alternative to completely decellularizing vessels als scaffolds. The  
45  
46 biomechanical properties are suitable, although both burst pressure and  
47  
48 Young's modulus need to be improved by conditioning the vessels in order to  
49  
50 obtain vessel grafts suitable for arterial conditions. Denuded HUV can be  
51  
52 reendothelialized in a perfusion bioreactor. The resulting neoendothelium is  
53  
54  
55  
56  
57  
58  
59  
60

1  
2  
3  
4  
5  
6  
7  
8  
9  
10  
11  
12  
13  
14  
15  
16  
17  
18  
19  
20  
21  
22  
23  
24  
25  
26  
27  
28  
29  
30  
31  
32  
33  
34  
35  
36  
37  
38  
39  
40  
41  
42  
43  
44  
45  
46  
47  
48  
49  
50  
51  
52  
53  
54  
55  
56  
57  
58  
59  
60

confluent and flow-resistant at venous flow rates.

## **Acknowledgements**

The authors wish to thank Klaus Falkner for performing the burst pressure analyses, Markus Niemeyer and Jürgen Burkhart for their help in umbilical cord logistics, and the midwives who rendered possible a continuous supply of umbilical cords. The skillful help of K. Bielenberg and H. Ebensberger in the lab and at the scanning electron microscope, respectively, was indispensable. This study was funded by Deutsche Forschungsgemeinschaft (BI 139/2-1, HA 4380/5-1, and LI 256/68-1).



## References

- 1  
2  
3  
4  
5  
6  
7  
8 Bjorling DE, Saban R, Tengowski MW, Gruel SM, Rao VK. 1992, Removal of  
9  
10 venous endothelium with air, *J Pharmacol Toxicol Methods*, **28**: 149-157  
11  
12  
13 Bordenave L, Fernandez P, Rémy-Zolghadri M, Villars S, Daculsi R, Midy D.  
14  
15 2005, In vitro endothelialized ePTFE prostheses: clinical update 20 years  
16  
17 after the first realization, *Clin Hemorheol Microcirc*, **33**: 227-234  
18  
19  
20 Campbell GR, Campbell JH. 2007, Development of tissue engineered vascular  
21  
22 grafts, *Curr Pharm Biotechnol*, **8**: 43-50  
23  
24  
25 Clarke DR, Lust RM, Sun YS, Black KS, Ollerenshaw JD. 2001, Transformation  
26  
27 of nonvascular acellular tissue matrices into durable vascular conduits, *Ann*  
28  
29 *Thorac Surg*, **71**: S433-S436  
30  
31  
32  
33 Crowston JG, Healey PR, Hopley C, Neilson G, Milverton EJ, Maloof A. 2004,  
34  
35 Water-mediated lysis of lens epithelial cells attached to lens capsule, *J*  
36  
37 *Cataract Refract Surg*, **30**: 1102-1106  
38  
39  
40 Daniel J, Abe K, McFetridge PS. 2005, Development of the human umbilical  
41  
42 vein scaffold for cardiovascular tissue engineering applications, *ASAIO J*,  
43  
44 **51**: 252-261  
45  
46  
47  
48 Dardik H, Wengerter K, Qin F, Pangilinan A, Silvestri F, Wolodiger F, Kahn M,  
49  
50 Sussman B, Ibrahim IM. 2002, Comparative decades of experience with  
51  
52 glutaraldehyde-tanned human umbilical cord vein graft for lower limb  
53  
54 revascularization: an analysis of 1275 cases, *J Vasc Surg*, **35**: 64-71  
55  
56  
57  
58  
59  
60

- 1  
2  
3 Derham C, Yow H, Ingram J, Fisher J, Ingham E, Korrosis SA, Homer-  
4  
5 Vanniasinkam S. 2008, Tissue engineering small-diameter vascular grafts:  
6 preparation of a biocompatible porcine ureteric scaffold, *Tissue Eng Part A*,  
7  
8 **14**: 1871-1882  
9  
10  
11  
12  
13 Fishman JA, Ryan GB, Karnovsky MJ. 1975, Endothelial regeneration in the rat  
14  
15 carotid artery and the significance of endothelial denudation in the  
16  
17 pathogenesis of myointimal thickening, *Lab Invest*, **32**: 339-351  
18  
19  
20  
21 Goldman S, Zadina K, Moritz T, Ovitt T, Sethi G, Copeland JG, Thottapurathu L,  
22  
23 Krasnicka B, Ellis N, Anderson RJ, Henderson W, VA Cooperative Study  
24  
25 Group #207/297/364. 2004, Long-term patency of saphenous vein and left  
26  
27 internal mammary artery grafts after coronary artery bypass surgery: results  
28  
29 from a Department of Veterans Affairs Cooperative Study, *J Am Coll*  
30  
31 *Cardiol*, **44**: 2149-2156  
32  
33  
34  
35  
36 Gui L, Muto A, Chan SA, Breuer CK, Niklason LE. 2009, Development of  
37  
38 decellularized human umbilical arteries as small-diameter vascular grafts,  
39  
40 *Tissue Eng Part A*, **15**: 2665-2676  
41  
42  
43  
44 Hoenicka M, Jacobs VR, Huber G, Schmid F, Birnbaum DE. 2008, Advantages  
45  
46 of human umbilical vein scaffolds derived from cesarean section vs. vaginal  
47  
48 delivery for vascular tissue engineering, *Biomaterials*, **29**: 1075-1084  
49  
50  
51  
52 Hoenicka M, Lehle K, Jacobs VR, Schmid FX, Birnbaum DE. 2007, Properties  
53  
54 of the human umbilical vein as a living scaffold for a tissue-engineered  
55  
56 vessel graft, *Tissue Eng*, **13**: 219-229  
57  
58  
59  
60

- 1  
2  
3 Hoenicka M, Wiedemann L, Puehler T, Hirt S, Birnbaum DE, Schmid C. 2010,  
4  
5 Effects of Shear Forces and Pressure on Blood Vessel Function and  
6  
7 Metabolism in a Perfusion Bioreactor, *Ann Biomed Eng*, **38**: 3706-3723  
8  
9  
10  
11 Hoenig MR, Campbell GR, Campbell JH. 2006, Vascular grafts and the  
12  
13 endothelium, *Endothelium*, **13**: 385-401  
14  
15  
16 Hoenig MR, Campbell GR, Rolfe BE, Campbell JH. 2005, Tissue-engineered  
17  
18 blood vessels: alternative to autologous grafts?, *Arterioscler Thromb Vasc*  
19  
20 *Biol*, **25**: 1128-1134  
21  
22  
23 Jaffe EA, Nachman RL, Becker CG, Minick CR. 1973, Culture of human  
24  
25 endothelial cells derived from umbilical veins. Identification by morphologic  
26  
27 and immunologic criteria, *J Clin Invest*, **52**: 2745-2756  
28  
29  
30  
31 Kong B, Foster LK, Foster DN. 2008, A method for the rapid isolation of virus  
32  
33 from cultured cells, *Biotechniques*, **44**: 97-99  
34  
35  
36 Lamm P, Juchem G, Milz S, Schuffenhauer M, Reichart B. 2001, Autologous  
37  
38 endothelialized vein allograft: a solution in the search for small-caliber  
39  
40 grafts in coronary artery bypass graft operations, *Circulation*, **104**: 1108-1114  
41  
42  
43 Li W, Zhang H, Wang P, Xi G, Wang H, Chen Y, Deng Z, Zhang Z, Huang T.  
44  
45 2008, Quantitative analysis of the microstructure of human umbilical vein  
46  
47 for assessing feasibility as vessel substitute, *Ann Vasc Surg*, **22**: 417-424  
48  
49  
50  
51 Mamode N, Scott RN. 1999, Graft type for femoro-popliteal bypass surgery,  
52  
53 *Cochrane Database Syst Rev*, : CD001487  
54  
55  
56 Narita Y, Kagami H, Matsunuma H, Murase Y, Ueda M, Ueda Y. 2008,  
57  
58  
59  
60

1  
2  
3 Decellularized ureter for tissue-engineered small-caliber vascular graft, *J*  
4  
5  
6 *Artif Organs*, **11**: 91-99  
7

8 Rigano S, Bozzo M, Padoan A, Mustoni P, Bellotti M, Galan HL, Ferrazzi E.  
9  
10 2008, Small size-specific umbilical vein diameter in severe growth  
11  
12 restricted fetuses that die in utero, *Prenat Diagn*, **28**: 908-913  
13  
14

15  
16 Zilla P, Bezuidenhout D, Human P. 2007, Prosthetic vascular grafts: wrong  
17  
18 models, wrong questions and no healing, *Biomaterials*, **28**: 5009-5027  
19  
20  
21  
22  
23  
24  
25  
26  
27  
28  
29  
30  
31  
32  
33  
34  
35  
36  
37  
38  
39  
40  
41  
42  
43  
44  
45  
46  
47  
48  
49  
50  
51  
52  
53  
54  
55  
56  
57  
58  
59  
60

For Peer Review

## Figure Legends

1  
2  
3  
4  
5  
6  
7  
8  
9  
10  
11  
12  
13  
14  
15  
16  
17  
18  
19  
20  
21  
22  
23  
24  
25  
26  
27  
28  
29  
30  
31  
32  
33  
34  
35  
36  
37  
38  
39  
40  
41  
42  
43  
44  
45  
46  
47  
48  
49  
50  
51  
52  
53  
54  
55  
56  
57  
58  
59  
60

Figure 1: Measurement of burst pressure. The stepper motor (1) drives the plunger of the syringe (2) at a constant rate. The luminal pressure is recorded via a pressure gauge (3). Two USB cameras (4, only one is shown for the sake of clarity) record the dimensions of the sample which is mounted in the vessel chamber (5). After filling the vessel with medium at the beginning of the experiment, the stopcock (6) is closed to allow buildup of pressure.

Figure 2: Seeding procedure. Cultured endothelial cells (1) are labelled (2), harvested, and transferred into a sterile syringe (3). Perfusion is stopped, whereas superfusion continues to run. The upstream perfusion stopcock (4) is closed, and the syringe is attached to the upstream port. After infusing the cell suspension into the sample, the downstream stopcock (5) is closed as well. Rotation (6) is then started to facilitate even distribution of the cells. The arrow (7) indicates the direction of medium flow during perfusion.

Figure 3: H&E stained thin sections of native and denuded HUV. (A) native HUV. (B) HUV denuded by luminal dehydration. (C) HUV denuded by collagenase treatment. (D-F) HUV denuded by osmotic lysis after 1, 3, and 5 min, respectively. Bar indicates 100  $\mu\text{m}$ .

1  
2  
3  
4  
5  
6  
7  
8  
9  
10  
11  
12  
13  
14  
15  
16  
17  
18  
19  
20  
21  
22  
23  
24  
25  
26  
27  
28  
29  
30  
31  
32  
33  
34  
35  
36  
37  
38  
39  
40  
41  
42  
43  
44  
45  
46  
47  
48  
49  
50  
51  
52  
53  
54  
55  
56  
57  
58  
59  
60

Figure 4: Representative uniaxial tensile testing experiments (Panel A) and burst pressure experiments (Panel B). Both samples were native HUV and are representative for 5-8 subjects.

Figure 5: Serotonin (5-HT) dose-response curves of native and denuded HUV. Filled circles: native HUV; open circles: collagenase-denuded HUV; filled triangles: gas-denuded HUV; open triangles: water-denuded HUV. \* significantly different from native controls (RM ANOVA,  $p=0.006$ ,  $n=7$ ).

Figure 6: Histological analysis of native and denuded HUV. aSMA,  $\alpha$ -smooth muscle actin stained with a specific antibody; Fibronectin, specific antibody; H&E, hematoxylin & eosin; Laminin, specific antibody; Resorcin, histochemical stain for elastic fibers; Sirius Red, histochemical stain for collagen. The images are representative for 9 independent experiments. Bar indicates 100  $\mu\text{m}$ .

1  
2  
3  
4  
5  
6  
7  
8  
9  
10  
11  
12  
13  
14  
15  
16  
17  
18  
19  
20  
21  
22  
23  
24  
25  
26  
27  
28  
29  
30  
31  
32  
33  
34  
35  
36  
37  
38  
39  
40  
41  
42  
43  
44  
45  
46  
47  
48  
49  
50  
51  
52  
53  
54  
55  
56  
57  
58  
59  
60

Figure 7: Fluorescence microscopy images of cross sections of denuded HUV seeded with endothelial cells. (A) HUVEC. (B) HSVEC. Images are representative for five independent experiments each. Bar indicates 100  $\mu\text{m}$ .

Figure 8: Scanning electron microscopy images of the luminal surfaces of (A) native HUV. (B) HUV denuded by dehydration. (C) denuded HUV seeded with allogeneic HUVEC, and (D) denuded HUV seeded with allogeneic HSVEC. Images are representative for three to five independent experiments.

Figure 9: CD31 and von Willebrand factor immunohistology. Gas-denuded HUV were devoid of any CD31 staining (A) whereas there was a confluent monolayer of CD31 positive cells (arrows) after seeding with HSVEC (B). Gas-denuded HUV showed a weak staining of von Willebrand factor in the subendothelial layer (arrow, C). After seeding with HSVEC, both the cells and the subendothelial layer stained positively for von Willebrand factor (arrows, D). Images are representative for 8 independent experiments. Bar indicates 100  $\mu\text{m}$ .

1  
2  
3  
4  
5  
6  
7  
8  
9  
10  
11  
12  
13  
14  
15  
16  
17  
18  
19  
20  
21  
22  
23  
24  
25  
26  
27  
28  
29  
30  
31  
32  
33  
34  
35  
36  
37  
38  
39  
40  
41  
42  
43  
44  
45  
46  
47  
48  
49  
50  
51  
52  
53  
54  
55  
56  
57  
58  
59  
60

For Peer Review



<b>treatment</b>	<b>failure force (N)</b>	<b>ultimate failure stress (kPa)</b>	<b>extrapolated burst pressure (kPa (mm Hg))</b>
native	2.53±0.54	8029±1714	268.8 (2016)
collagenase	1.58±0.36 *	5014±1142 *	167.9 (1259) *
gas	2.35±0.28	7458±889	249.7 (1873)
water	2.61±0.52	8283±1650	277.3 (2080)

Table 1: Tensile testing data of native and denuded HUV. \* significantly different from native HUV (RM ANOVA, p=0.007, n=5).

treatment	contractile force 150 mM KCl (mN)	maximum contractile force 5-HT (mN)	log(EC <sub>50</sub> ) 5-HT (M)	reductive capacity (OD <sub>490</sub> )
native	45.05±26.27	62.60±29.36	-8.44±0.63	0.76±0.33
collagenase	16.89±12.90*	30.00±21.09 <sup>§</sup>	-7.84±1.00 <sup>†</sup>	0.64±0.18
gas	37.55±18.75	58.39±27.17	-8.55±0.60	0.66±0.16
water	18.61±20.61*	32.87±30.31 <sup>§</sup>	-8.03±0.58	0.66±0.14

Table 2: Organ bath and tetrazolium dye reduction data of native and denuded HUV. \* significantly different from native HUV (RM ANOVA, p=0.005, n=7).

<sup>§</sup> significantly different from native HUV (RM ANOVA, p=0.001, n=7).

<sup>†</sup> significantly different from native HUV (RM ANOVA, p=0.006, n=7).

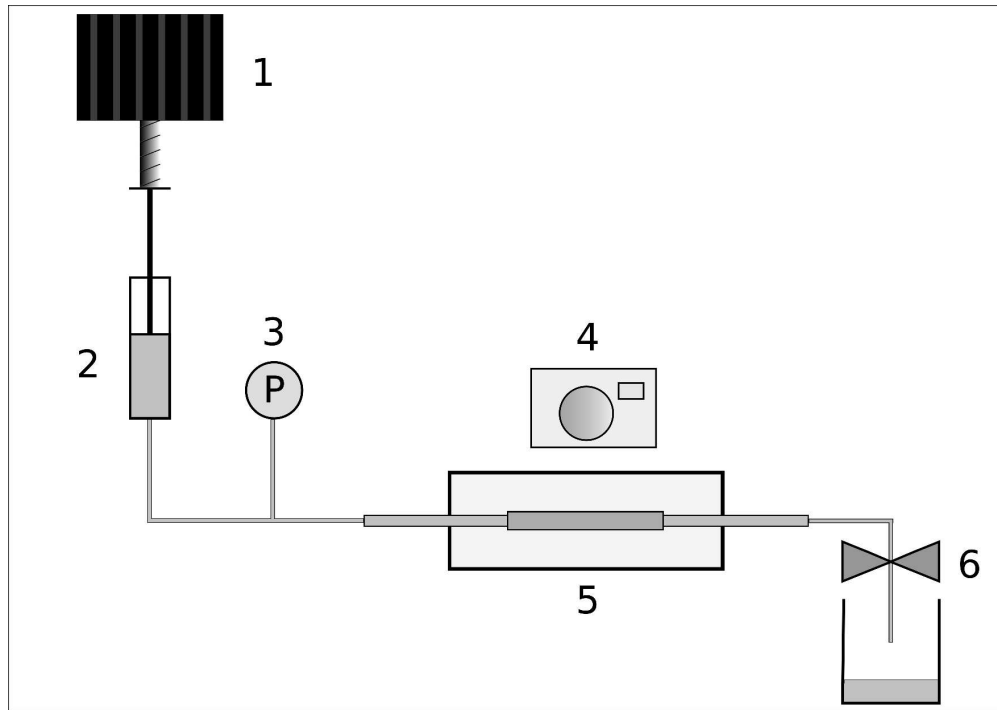


Figure 1: Measurement of burst pressure. The stepper motor (1) drives the plunger of the syringe (2) at a constant rate. The luminal pressure is recorded via a pressure gauge (3). Two USB cameras (4, only one is shown for the sake of clarity) record the dimensions of the sample which is mounted in the vessel chamber (5). After filling the vessel with medium at the beginning of the experiment, the stopcock (6) is closed to allow buildup of pressure.

297x210mm (300 x 300 DPI)

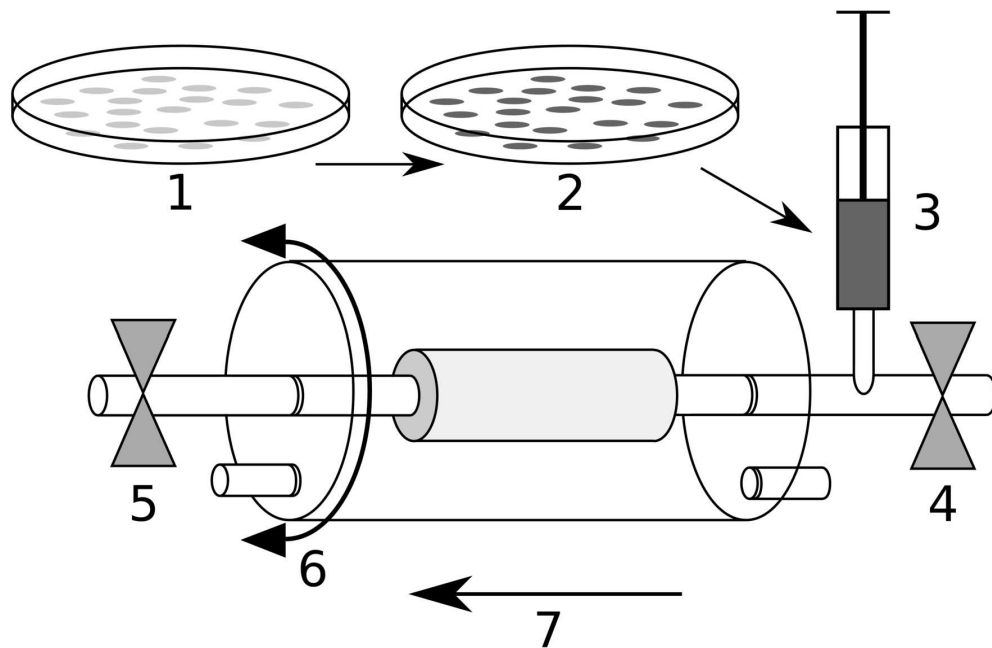


Figure 2: Seeding procedure. Cultured endothelial cells (1) are labelled (2), harvested, and transferred into a sterile syringe (3). Perfusion is stopped, whereas superfusion continues to run. The upstream perfusion stopcock (4) is closed, and the syringe is attached to the upstream port. After infusing the cell suspension into the sample, the downstream stopcock (5) is closed as well. Rotation (6) is then started to facilitate even distribution of the cells. The arrow (7) indicates the direction of medium flow during perfusion.

150x97mm (300 x 300 DPI)

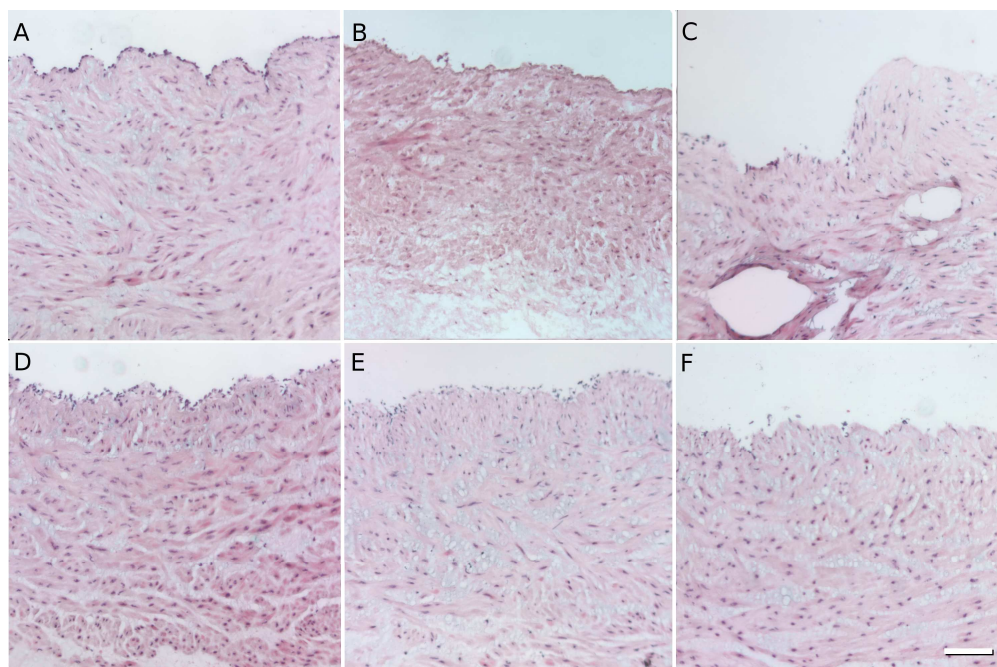


Figure 3: H&E stained thin sections of native and denuded HUV. (A) native HUV. (B) HUV denuded by luminal dehydration. (C) HUV denuded by collagenase treatment. (D-F) HUV denuded by osmotic lysis after 1, 3, and 5 min, respectively. Bar indicates 100  $\mu\text{m}$ .

1058x702mm (72 x 72 DPI)

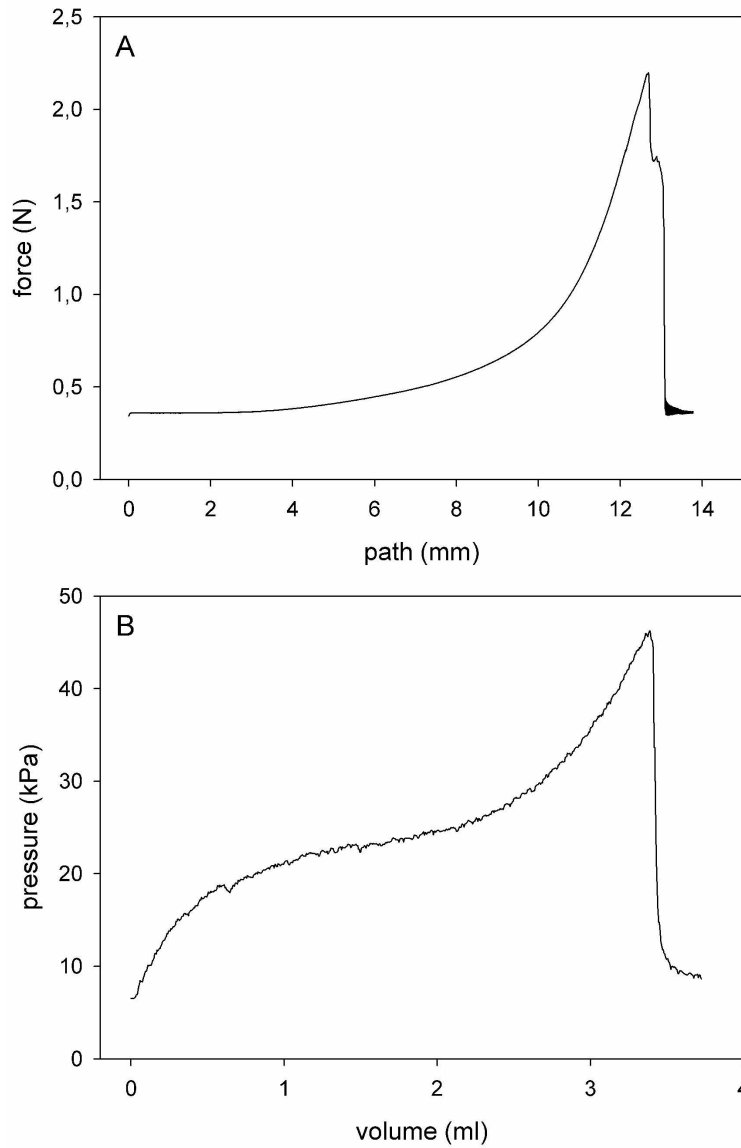


Figure 4: Representative uniaxial tensile testing experiments (Panel A) and burst pressure experiments (Panel B). Both samples were native HUV and are representative for 5-8 subjects. 601x932mm (150 x 150 DPI)

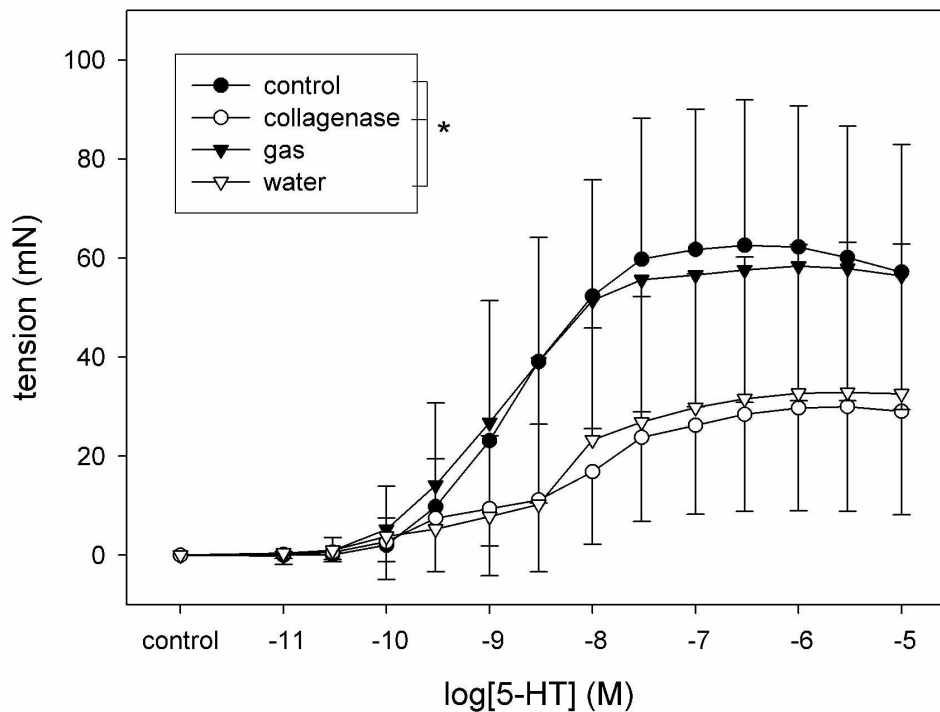
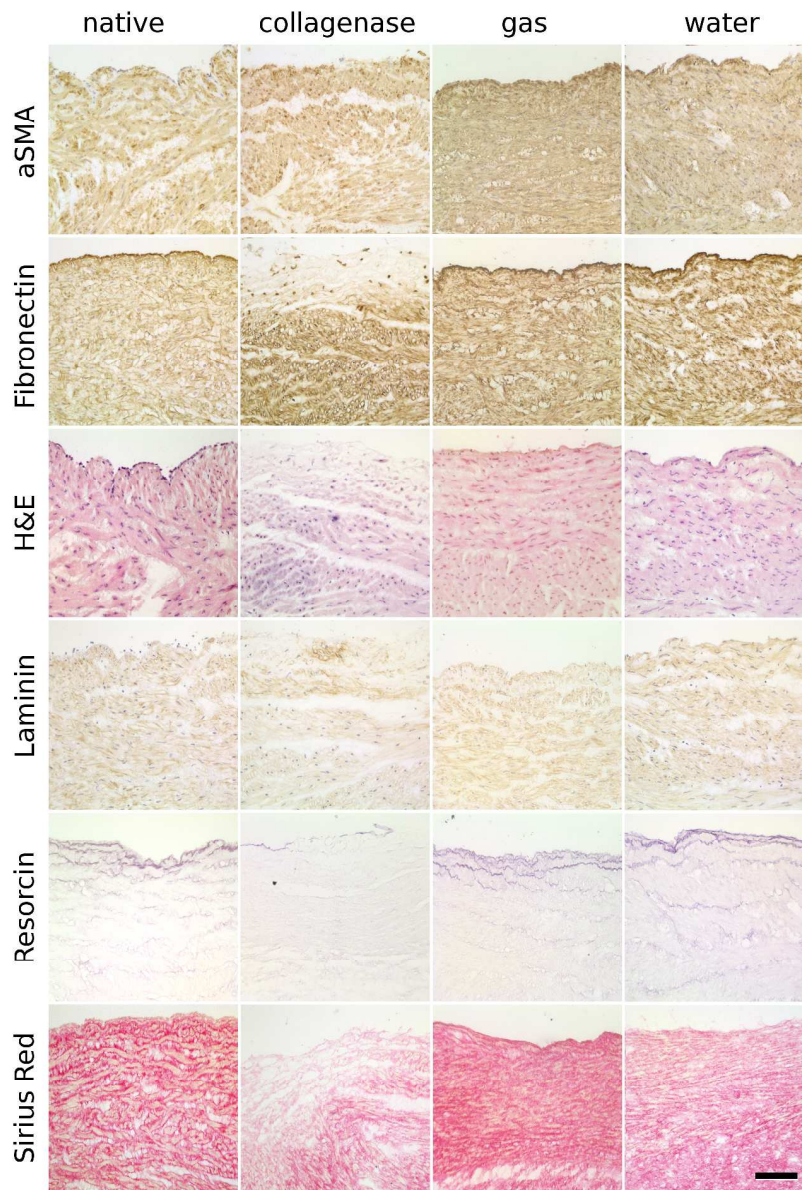


Figure 5: Serotonin (5-HT) dose-response curves of native and denuded HUVEC. Filled circles: native HUVEC; open circles: collagenase-denuded HUVEC; filled triangles: gas-denuded HUVEC; open triangles: water-denuded HUVEC. \* significantly different from native controls (RM ANOVA,  $p=0.006$ ,  $n=7$ ).  
606x483mm (150 x 150 DPI)



46  
47  
48  
49  
50  
51  
52  
53  
54  
55  
56  
57  
58  
59  
60

Figure 6: Histological analysis of native and denuded HUV. aSMA,  $\alpha$ -smooth muscle actin stained with a specific antibody; Fibronectin, specific antibody; H&E, hematoxylin & eosin; Laminin, specific antibody; Resorcin, histochemical stain for elastic fibers; Sirius Red, histochemical stain for collagen. The images are representative for 9 independent experiments. Bar indicates 100  $\mu$ m.  
913x1342mm (72 x 72 DPI)



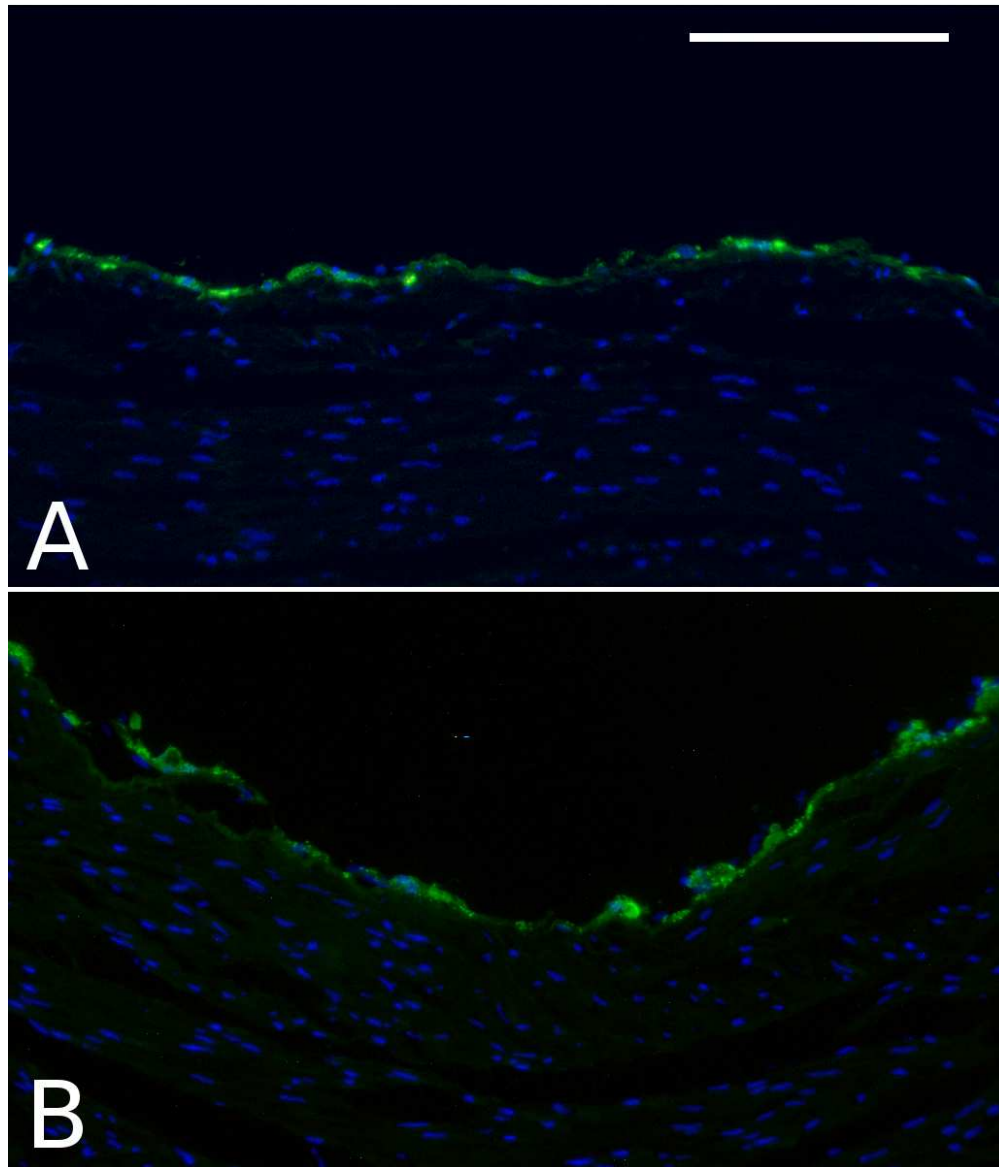


Figure 7: Fluorescence microscopy images of cross sections of denuded HUV seeded with endothelial cells. (A) HUVEC. (B) HSVEC. Images are representative for five independent experiments each. Bar indicates 100  $\mu\text{m}$ .

1  
2  
3  
4  
5  
6  
7  
8  
9  
10  
11  
12  
13  
14  
15  
16  
17  
18  
19  
20  
21  
22  
23  
24  
25  
26  
27  
28  
29  
30  
31  
32  
33  
34  
35  
36  
37  
38  
39  
40  
41  
42  
43  
44  
45  
46  
47  
48  
49  
50  
51  
52  
53  
54  
55  
56  
57  
58  
59  
60

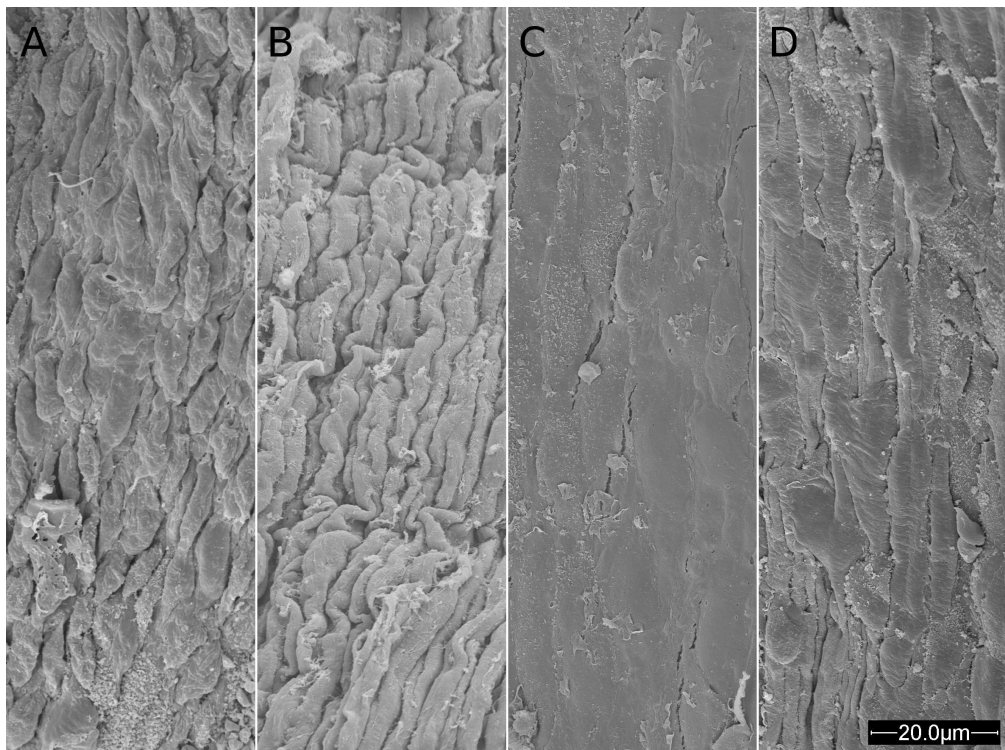


Figure 8: Scanning electron microscopy images of the luminal surfaces of (A) native HUV. (B) HUV denuded by dehydration. (C) denuded HUV seeded with allogeneic HUVEC, and (D) denuded HUV seeded with allogeneic HSVEC. Images are representative for three to five independent experiments.

Review

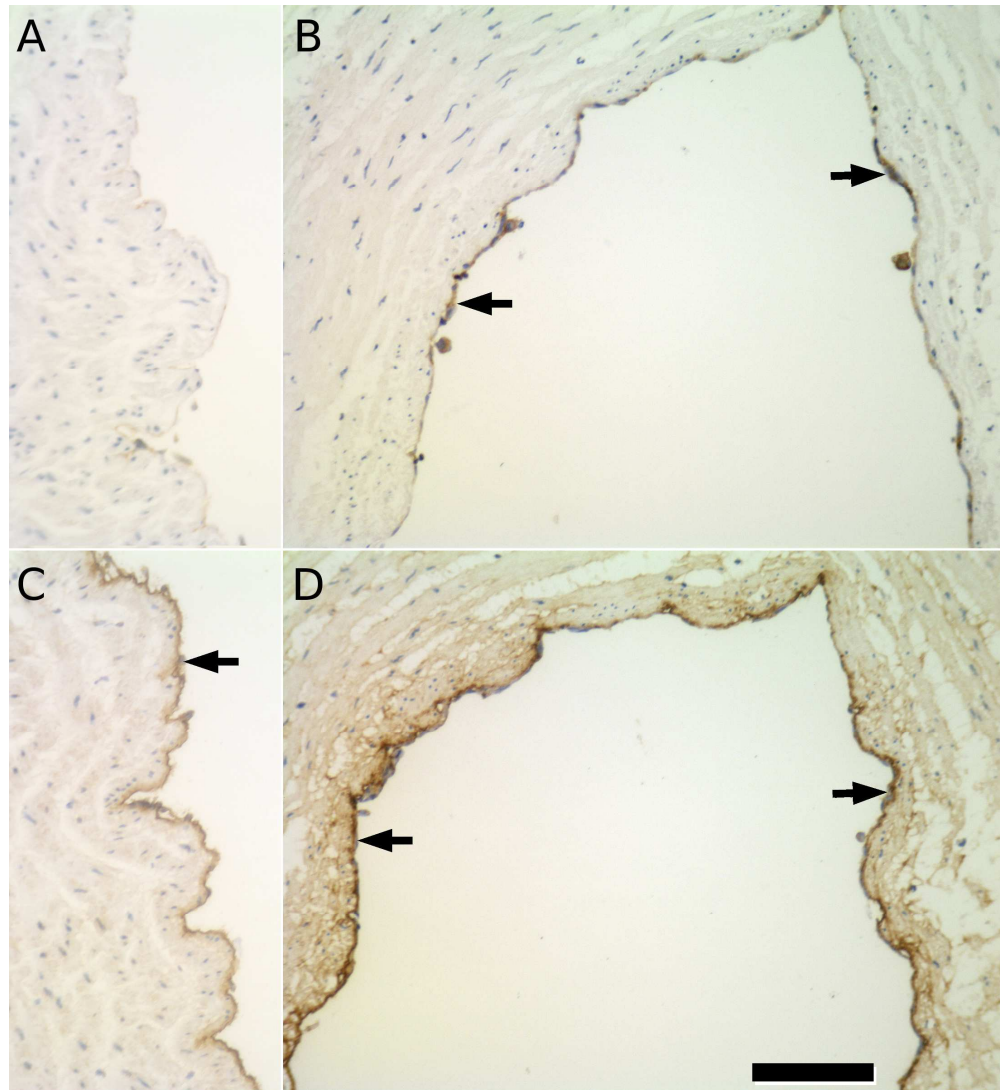


Figure 9: CD31 and von Willebrand factor immunohistology. Gas-denuded HUV were devoid of any CD31 staining (A) whereas there was a confluent monolayer of CD31 positive cells (arrows) after seeding with HSVEC (B). Gas-denuded HUV showed a weak staining of von Willebrand factor in the subendothelial layer (arrow, C). After seeding with HSVEC, both the cells and the subendothelial layer stained positively for von Willebrand factor (arrows, D). Images are representative for 8 independent experiments. Bar indicates 100  $\mu$ m.